Published in final edited form as:
Clin Chem. 2012 June ; 58(6): 1010–1018. doi:10.1373/clinchem.2011.179200.

Clinical Measurement of von Willebrand Factor by Fluorescence Correlation Spectroscopy

Richard Torres[1,2], **Jonathan R. Genzen**[3], and **Michael J. Levene**[1,*]

[1]Department of Biomedical Engineering, Yale University and Yale School of Medicine, New Haven, CT

[2]Department of Laboratory Medicine, Yale University and Yale School of Medicine, New Haven, CT

[3]Department of Pathology and Laboratory Medicine, Weill Cornell Medical College, New York Presbyterian Hospital, New York, NY

Abstract

BACKGROUND—Identification of von Willebrand factor (vWF) abnormalities in a variety of conditions is hampered by the limitations of currently available diagnostic tests. Although direct multimer visualization by immunoelectrophoresis is a commonly used method, it is impractical as a routine clinical test. In this study, we used a biophysical analysis tool, fluorescence correlation spectroscopy (FCS), to measure vWF distributions. The goals were to develop a method that is quicker and simpler than vWF gel electrophoresis and to evaluate the potential of FCS as a clinical diagnostic technique.

METHODS—We analyzed plasma from 12 patients with type 1 von Willebrand disease (vWD), 14 patients with type 2 vWD, and 10 healthy controls using a fluctuation-based immunoassay approach.

RESULTS—FCS enabled identification and proper classification of type 1 and type 2 vWD, producing quantitative results that correspond to qualitative gel multimer patterns. FCS required minimal sample preparation and only a 5-min analysis time.

CONCLUSIONS—This study represents the first implementation of FCS for clinical diagnostics directly on human plasma. The technique shows potential for further vWF studies and as a generally applicable laboratory test method.

The protein von Willebrand factor (vWF)[4] functions as a recruiter, tether, and activator of platelets and as the protective carrier for factor VIII. It is normally present in plasma as a

*Address correspondence to this author at: P.O. Box 208260, New Haven, CT 06520. michael.levene@yale.edu. .

Author Contributions: All authors confirmed they have contributed to the intellectual content of this paper and have met the following 3 requirements: (a) significant contributions to the conception and design, acquisition of data, or analysis and interpretation of data; (b) drafting or revising the article for intellectual content; and (c) final approval of the published article.

Authors' Disclosures or Potential Conflicts of Interest: Upon manuscript submission, all authors completed the author disclosure form. Disclosures and/or potential conflicts of interest:

Employment or Leadership: None declared.

Consultant or Advisory Role: None declared.

Stock Ownership: None declared.

Honoraria: None declared.

Expert Testimony: None declared.

distribution of multimers containing anywhere from 2 to 40 or more vWF monomers. Abnormalities in vWF activity, most often related to abnormal concentration or multimer distribution, are the incident cause of the group of coagulopathies known as von Willebrand disease (vWD) (1, 2). As a group, vWD is considered to be the most common inherited coagulation disorder. Abnormalities in vWF are also responsible for secondary bleeding conditions, such as in acquired vWD, and are associated with inherited and acquired thrombotic states, such as the procoagulant disease known as thrombotic thrombo-cytopenia purpura. In addition, several common conditions have been known to affect vWF distributions including coronary artery disease, pregnancy, cancer, sepsis, diabetes, autoimmune disease, and others (3-5). Despite its importance in inherited and acquired bleeding disorders, and the mounting evidence for its role in thrombotic disease, routine evaluation is hampered by the limitations of currently available laboratory tests.

Limitations in vWF Testing

The main clinical subclassification of vWF abnormalities is based on whether the deficiency is purely a quantitative one (type 1 vWD) or includes a functional component (type 2 vWD). Type 2 vWD is most often related to a decrease in the concentration of larger multimers, which have the highest ability to bind collagen and recruit and activate platelets. A third type (type 3 vWD) is characterized by complete or near-complete absence of vWF, which is fortunately rare.

The groupings above have clinical consequences that relate to therapy and prognosis. In type 1 vWD, patients may receive the vasopressin analog 1-deamino-[8-D-arginine]-vasopressin (DDAVP), which stimulates preferentially large multimer secretion from endothelial cells (6) and often provides sufficient functional capacity for adequate hemostasis. Type 2 vWD is much more likely to require the administration of vWF concentrate. Antibody-based quantification of vWF antigen (vWF:Ag) concentration does not provide information regarding the relative multimer size distribution and cannot be used independently to subclassify vWF abnormalities.

Functional tests used for classification, such as ristocetin cofactor activity (vWF:RCof) and the collagen-binding assay (vWF:CB), suffer from poor reproducibility, limited reportable ranges, and lack of standardization. The gold standard for multimer visualization, gel electrophoresis, is a cumbersome, non-quantitative, and time-consuming assay primarily available only from reference laboratories. Additional diagnostic challenges associated with current vWF laboratory testing methods have been recently reviewed (7, 8).

Fluorescence Correlation Spectroscopy

Fluorescence correlation spectroscopy (FCS) measures the absolute concentration and mobility of fluorescent species as they diffuse through a well-defined observation volume. It has not been previously applied to clinical testing in human plasma. FCS is well suited for this type of testing in that it is rapid, simple to perform, and has a low cost per test. FCS can be performed without washing steps, with volume measurements that are optically defined, and with very small amounts of testing sample and reagents.

In FCS, when on average only a few molecules are present in a given observation volume, fluctuations in the actual number follow predictable Poisson statistics [see references (9-11) for more detailed description]. Comparison of fluctuations in the fluorescence signal to the

[4]Nonstandard abbreviations: vWF, von Willebrand factor; vWD, von Willebrand disease; DDAVP, 1-deamino-[8-D-arginine]-vasopressin; vWF:Ag, vWF antigen; vWF:RCof, ristocetin cofactor activity; vWF:CB, collagen-binding assay; FCS, fluorescence correlation spectroscopy; TRITC, tetramethyl-rhodamine-isothiocyanate.

mean fluorescence signal yields the mean number of molecules in the observation volume. The typical time scale of the fluctuations corresponds to the time it takes molecules to diffuse through the observation volume, and can therefore be related to the diffusivity of the molecules, a property that is proportional to molecule size.

In practice, a laser focused to a diffraction-limited spot by a microscope objective combined with a confocal detection pinhole defines the observation volume for FCS (Fig. 1A). The basic instrument is relatively simple and inexpensive to build, consisting of a microscope objective, a high-sensitivity detector, and a specialized computer card to plot the autocorrelation of the fluorescence signal, $G(\tau)$, vs the correlation delay time τ (Fig. 1B). This curve can be fit to a function derived from the shape of the observation volume, yielding the mean number of molecules per volume, N, and the residence time (mean time of diffusion through observation volume), τ_d. For the typical confocal excitation profile, one can assume a 3-dimensional gaussian observation profile such that:

$$G(\tau) = 1 + \frac{\left(1 - f_t + f_t e^{-(\tau/\tau_t)}\right)}{(1 - f_t)} \frac{1}{N} \left(\frac{1}{1+\frac{\tau}{\tau_d}}\right)\left(\frac{1}{1+\frac{\tau}{S^2\tau_d}}\right)^{1/2}, \quad (1)$$

where τ is the correlation time, S is the structure parameter (ratio of radial to axial observation volume diameters), τ_t is the triplet lifetime, and f_t corresponds to the triplet state fraction. The residence time, τ_d, is related to the diffusion coefficient, D, by the Stokes-Einstein equation via the diameter of the observation volume in the x,y direction $w_{x,y}$: $\tau_d = \frac{w_{x,y}^2}{4D}$. Thus, the concentration of fluorescent molecules and their diffusion coefficient can be determined directly from the fluctuations in emitted photons over time.

FCS for vWF Measurement

The goal of this report is to examine whether FCS can address some of the limitations of current methods for vWF assessment, looking to develop a more practical tool than multimer gel analysis for measuring vWF size distributions in bleeding and clotting disorders. In this study, we used FCS for the measurement of vWF multimers in plasma from a cohort of patients with vWF test results within reference intervals and from patients with type 1 and type 2 vWD. We analyzed how the quantity and quality of vWF substrate affects measureable parameters in the FCS assay and present an approach that allows adequate subclassification of vWD with this simple-to-implement method.

Methods

EXPERIMENTAL DESIGN AND SAMPLE SELECTION

Using institutional review board-approved protocols, we identified samples for analysis from vWF:Ag, vWF:RCof, factor VIII, and multimer gel analysis data generated during routine vWD testing at Yale-New Haven Hospital and Weill Cornell Medical College. Twenty-six samples from patients who fulfilled the respective laboratory director's criteria for von Willebrand disease (12 type 1 and 14 type 2) were selected on the basis of unequivocally low values in vWF:Ag (<50%), vWF:RCof (<50%), and/or antigen-to-activity ratio (<0.5). Although current recommendations for characterization as vWD vary, these concentrations correspond to the reference values used clinically at the testing site, and values below 50% are associated with progressively increased risk of excessive bleeding relative to average healthy controls regardless of cause. Samples were also collected from 1 patient who underwent a therapeutic DDAVP trial. Ten apparently healthy patients with all vWF values within reference intervals (75% < vWF:Ag <150%, 75% < vWF:RCof <150%)

and confirmed normal multimer analyses were randomly selected for comparison. Antigen and activity percentage units refer to a normalized pooled standard representing 100%, equivalent to 100 U/dL, against which reference standards used for calibration are measured (Diagnostica-Stago).

TRADITIONAL vWF TESTING

Sample collection and testing were performed by standard procedures as described in the Data Supplement, which accompanies the online version of this article at http://www.clinchem.org/content/vol58/issue6.

vWF TESTING BY FCS

Samples were thawed at 37 °C and then incubated with tetramethyl-rhodamine-isothiocyanate (TRITC)-labeled monoclonal anti-vWF antibody directed to the D3 domain (Santa Cruz Biotechnology) at a final concentration of 20 nmol/L for 30 min at room temperature. We diluted 40 μL plasma 1:1 with antibody-containing phosphate buffer at pH 7.1. This dilution ensures a near-normalization of the viscosity to that of saline (12). We placed 40 μL incubated sample atop a #0 coverslip (Thermo Fisher) and analyzed it in a Confocor 2 fluorescence correlation microscope (Zeiss) at room temperature with a 40× 1.2-NA coverslip-corrected water immersion objective (Zeiss) by standard FCS procedures (10, 13). Excitation was done with a helium-neon laser at 543 nm, 543 nm dichroic mirror, and 560-615 nm emission filter. Pinhole diameter was 78 μm. Ten runs of 30 s were averaged for each sample.

DATA ANALYSIS

We fitted correlation curves from tagged antibody at 50 nmol/L in phosphate buffer to a 1-component FCS equation with a triplet term (Eq. 1). The structure parameter and observation volume were derived from fits of tetramethylrhodamine dye at 100 nmol/L concentration. The triplet time (τ_t, approximately 10 μs) and antibody diffusion time (τ_d, approximately 320 μs) were derived from fits of TRITC-labeled antibody at 50 nmol/L. The reduced χ^2/degrees of freedom (χ^2/DoF) was always on the order of 1×10^{-6}. Raw FCS curves were fitted online on Confocor or offline with Origin software (OriginLabA). Triplet fractions (f_t) ranged from 8% to 10%. Autocorrelation curves of samples without added fluorescent antibody showed background plasma counts <10% of antibody fluorescence, with a high triplet fraction and an effective mean diffusion time of approximately 120 μs, dim and of fast enough diffusion time to be neglected from the comparison of mean diffusion time and component ratios in FCS curves.

The autocorrelation curves obtained from FCS analysis of patient samples incubated with fluorescently tagged anti-vWF were fitted to a 2-component FCS equation such that:

$$G_{\text{total}}(\tau) = [a_{\text{free}} \times G_{\text{free}}(\tau, \tau_{\text{free}})] + [a_{\text{bound}} \times G_{\text{bound}}(\tau, \tau_{\text{bound}})] \quad (2)$$

where $G_{\text{free}}(\tau)$ and $G_{\text{bound}}(\tau)$ are the normalized autocorrelation functions for the free- and bound-antibody components, and a_{free} and a_{bound} are their relative contributions (corresponding fraction) to the correlation function $G_{\text{total}}(\tau)$. The relative brightness of free and bound components affects the proportionality between a_{free} and a_{bound} and therefore these represent "effective" fractions, corresponding to the proportion if the brightness was equal between subsets (also see the online Data Supplement). Although this is not expected to be the case in these experiments, this use of effective bound fractions allowed adequate discrimination, simplified the analysis, and improved the robustness of the fits considerably. The diffusion time (τ_{free}) of the free component was fixed at the measured τ_d of antibody alone (320 μs, appropriate for the expected molecular weight of 140 kDa and an observation

volume diameter ω_{x-y} of 265 nm, calculated from dye diffusion times). For individual 2-component fits, the χ^2/DoF was always $<2 \times 10^{-5}$. We obtained the mean nonantibody diffusion time and an effective fraction of antibody bound directly from this 2-component fit. We generated normalized curves from the *G (0)* calculated on the raw 2-component fits for clearer visual comparison of FCS curve shapes. These normalized curves use an alternate form of Eq. 1 that omits the leading 1.

Results

To demonstrate the effect of vWF concentration on FCS curves, we analyzed serial saline dilutions of a normal sample. The FCS curves from these dilutions show a progressive shift toward longer mean diffusion times (curves shift to the right) with higher vWF concentrations (Fig. 2A), as might be expected with increasing binding of antibody. A global two-component fit for the dilution curves, with 1 diffusion time fixed at the antibody diffusion time, describes the data well (Fig. 2A; overall fit χ^2/DoF = 4.0×10^{-5}, R^2 = 0.9995). We calculated proportional increases in the percentage of the curve represented by the longer diffusion time (Fig. 2B). We observed an excellent linear correlation between the antigen concentration of the dilution and the effective fraction of antibody bound to vWF as determined from the 2-component fits. These results indicate that a 2-component fit is able to extract an effective bound percentage from the FCS curves, and it is consistent with the interpretation that we are operating in the concentration range where antibody is not fully bound. The correlation (Fig. 2B) also demonstrates a leveling off at the highest vWF:Ag concentrations, as would be expected when available vWF antibody binding sites approach the antibody concentration.

By contrast, differences in the mean diffusion time between type 1 and type 2 vWD patient samples were not directly proportional to antigen concentration. Fig. 3A shows a representative comparison of normalized FCS curves from a patient with a type 1 vWD pattern (normal multimer distribution, reduced vWF:Ag concentrations), a patient with a type 2 vWD pattern (reduced mean multimer size and higher vWF:Ag concentrations higher than the type 1 sample), and a healthy control. There is an expected shift toward shorter mean diffusion times in the type 2 vWD sample, which contained only the smallest vWF multimers as seen in multimer gels (Fig. 3B). Distinction of this type 2 vWD sample from a very severe type 1 vWD sample, which would also have a fast mean diffusion time, may not be readily apparent by visual inspection of the FCS curves alone. However, the 2-component fit disentangles the effects of changes in overall vWF concentration from those of the vWF distribution, now represented by the calculated relative proportion of free and bound antibody and by the effective mean diffusion time of the bound antibody component (designated by arrows in Fig. 4).

The 26 samples with vWF abnormalities also tested by FCS are described in Table 1. There is significant overlap between type 1 vWD and type 2 vWD patient samples for vWF:Ag and vWF:RCof results, making individual tests insufficient for an accurate classification. The effective percentage of slowly diffusing antibody and the mean diffusion time of this bound component was calculated from 2-component fits of the FCS curve. As shown in Fig. 4, specimens from healthy controls, type 1 vWD patients, and type 2 vWD patients cluster into 3 separate groups when plotted for these 2 parameters. As physiologically expected, type 1 vWD patients show an effective bound fraction (percentage bound) that is lower than that of controls, but with a mean diffusion of the bound component (bound τ) that is in the normal range. Type 2 vWD patients show an effective bound fraction that is in the range of type 1 vWD patients (as they have largely overlapping total antigen concentrations; see Table 1), but with a reduced mean diffusion of the bound component, reflective of the lack of large multimers that defines most type 2 vWD cases. Finally, 3 samples with clinically

established relatively mild acquired type 2 deficiency, but with vWF:Ag concentrations higher than 50%, appropriately demonstrated a high bound antibody percentage but with a small mean multimer size (Fig. 4). The overall results provide a rational basis for disease classification by FCS analysis.

Additional experiments were performed with samples from a type 1 vWD patient taken at baseline, 1 h, and 4 h after administration of DDAVP, a compound that stimulates endothelial cell release of ultra-large multimers, which are subsequently cleaved in the circulation to achieve the steady-state distributions observed. There are corresponding changes noted with FCS with slower diffusion at 1 h and partial return to baseline at 4 h (Fig. 5A). Two-component fits (Fig. 5B) yielded a pattern of DDAVP response consistent at 1 h with an increase in the quantity (effective percentage bound) and mean size (mean bound diffusion time) of the multimer distribution. When compared to 1 h, the 4-hour sample shows a decrease in the mean size with only a small decrease in total antigen. The antigen assays are consistent with this result (Table 1). The cofactor activity assays are also generally consistent with this result, but are difficult to interpret because activity is affected by the antigen concentration in such a way that multimer size is not easily inferred. The gel multimer analysis is also not easily quantifiable for this DDAVP response (Fig. 5C).

Discussion

NEED FOR ALTERNATIVE vWF METHODS

Current functional tests for vWF include the ristocetin cofactor activity assay and the collagen-binding assay. The vWF:RCof assay measures the ability of patient-derived vWF to agglutinate formalin-fixed healthy donor platelets. The vWF:CB assay measures the ability of patient vWF to bind collagen affixed to reaction wells. Both tests have been designed to be sensitive to the distribution of vWF multimers, but they suffer from important limitations (14). The vWF:RCof assay has limited sensitivity and poor reproducibility. Furthermore, there is disagreement about the optimal threshold for disease classification. Repeated runs of vWF:RCof are needed for adequate precision, and a relatively high lower end of the reportable range observed with some vWF:RCof assays can render it useless in patients with moderate antigen deficiencies (<20%), as exemplified by several samples listed in Table 1. The utility of the other functional assay, vWF:CB, is limited by the lack of adequate reagent standardization and variability in the types of collagen used. The lack of a reference standard for this test makes extensive internal validations necessary. Additionally, data are lacking on the reliability of both the vWF:RCof and vWF:CB assays in detecting clinically relevant increases in large vWF multimers.

The only method in current clinical use to directly visualize vWF multimers remains gel electrophoresis, which suffers from high technical complexity and a time-consuming nature (15). The use of gel electrophoresis for vWF multimers is generally restricted to reference laboratories, most often for the second-stage evaluation of vWD. A typical setup requires overnight electrophoretic runs of denatured protein in 1%-2% agarose gel. Detection is often completed through radio-immunoblotting, creating additional difficulties associated with the use of radiation-containing reagents in the clinical laboratory. Variability in results from gel to gel is another confounding factor inherent to this technique, particularly when attempting to use these results to quantify multimer distributions. Whereas minor stimuli may cause rapid, significant changes to the circulating concentrations of vWF protein (and to multimer distributions for which repeated measurements could aid in diagnosis and risk assessment), the challenges associated with vWF gel electrophoresis procedures make the technique impractical for use in this manner.

FCS FOR vWF CLINICAL TESTING

Although it has found widespread use within the biophysics community since its first implementation almost 40 years ago, FCS has not been widely used for clinically relevant diagnostics. One factor affecting the application of FCS to immunoassay-type clinical analysis is that >6-fold changes in molecular weight are typically required for shifts in mean diffusion time to be reliably detected. However, given that functional characteristics of vWF depend on the relative size of multimers present, and that the multimers achieve such large sizes, FCS is particularly well suited for vWF measurement. Additional discussion on multimeric protein analysis via FCS is presented in the online Data Supplement.

In the present report, experimental FCS measurements of vWF in patients with type 1 and type 2 vWD followed in perfect agreement with the qualitative results from multimer gel analysis. Even if the measured bound fraction and bound mean diffusion times are only surrogate markers of the actual multimer size distribution, in contrast to labor-intensive gel electrophoresis, the FCS method was able to obtain clinically useful data with only 30-min antibody incubation and 5-min analysis time. The cost per test was minimal, and execution of the analysis was straightforward and quick. Also, the end points were easily comparable numerical results.

As in traditional gel multimer analysis, distinction of certain type 2 vWD subtypes (such as type 2B and type 2M), would require testing in addition to multimer analysis for accurate clinical classification. The overall utility of multimer analysis, however, would still be augmented by a simpler and faster method that provides the most relevant information, i.e., the effective mean multimer size and overall amount of antigen present. The quantitative nature, short analysis time, and potential for very low cost per test in FCS would make it possible to obtain these parameters on virtually every sample for which antigen and activity are being measured, as well as potentially obviate the need for slow, laborious, nonquantitative multimer gel testing, which requires subjective interpretation.

DDAVP TRIAL ANALYSIS BY FCS

The DDAVP trial demonstrates how FCS with 2-component fits can help characterize the response to therapy. Mechanisms of type 1 vWD vary and include decreased synthesis, increased clearance, and/or increased breakdown of vWF. In addition to providing therapeutic prognosis, 4-h DDAVP trials can sometimes help elucidate the underlying defect (e.g., the rapid clearance of type 1 Vincenza). Theoretically, multimer distribution changes in response to DDAVP are affected by the specific vWF abnormality, i.e., secretion, multimerization, cleavage, etc. Thus, there exists an opportunity to gain additional insight into the mechanisms responsible for vWF deficiencies during a DDAVP trial by looking at multimer distribution time-courses. The current limitations of multimer gels, such as lack of reliable quantitative data and the other afore-mentioned difficulties, make this investigation currently impractical. Whether FCS is indeed capable of yielding complementary information relevant to the mechanism responsible for vWF deficiency in individual patients should be explored further, as it could have direct implications in the therapeutic approach. Because of its ability to produce numerical results sensitive to changes in large multimers, FCS analysis may similarly be useful in assessing thrombotic risk and/or extent of abnormalities in conditions known to be associated with hypercoagulability.

Conclusions

The findings presented in this report show that FCS can be used to measure parameters that reflect vWF distributions in patient samples and, through these measurements, can produce clinically meaningful results. To our knowledge, it represents the first medical diagnostic

application of this biophysical technique directly on human plasma. Fluctuation-based immunoassays could find a role in the routine evaluation of vWF, in both vWD diagnosis and the assessment of therapeutic response. Implementation in clinical use will require further characterization of its analytical capabilities. We also believe that establishing FCS as a clinically relevant technique would create opportunities for expansion of this simple-to-implement approach to address a variety of shortcomings in current clinical laboratory techniques.

Supplementary Material

Refer to Web version on PubMed Central for supplementary material.

Acknowledgments

The authors thank Dr. David Andrews from University of Miami Miller School of Medicine for helping perform multimeric gel analysis and providing the gel scans presented here. We also thank Dr. Brian R. Smith for participating in the development of the research concept.

Research Funding: R. Torres, partial salary support from the National Center for Research Resources (NCRR), a component of the NIH, NIH Roadmap for Medical Research, and partial salary support from the National Heart, Lung, and Blood Institute (NHLBI) of the NIH; M.J. Levene, partial salary support and Clinical and Translational Science Awards grant UL1 RR024139 from NCRR and partial salary support and grant R21 HL094796 from NHLBI.

Role of Sponsor: The funding organizations played no role in the design of study, choice of enrolled patients, review and interpretation of data, or preparation or approval of manuscript.

References

1. Sadler J, Budde U, Eickenboom J, Favaloro E, Hill F, Holmberg L, et al. Update on the pathophysiology and classification of von Willebrand disease: a report of the subcommittee on von Willebrand factor. J Thromb Haemost. 2006; 4:2103–14. [PubMed: 16889557]
2. Torres R, Fedoriw Y. Laboratory testing for von Willebrand disease: toward a mechanism-based classification. Clin Lab Med. 2009; 29:193–228. [PubMed: 19665675]
3. Ono T, Mimuro J, Madoiwa S, Soejima K, Kashiwakura Y, Ishiwata A, et al. Severe secondary deficiency of von Willebrand factor cleaving protease (ADAMTS13) in patients with sepsis-induced disseminated intravascular coagulation: its correlation to development of renal failure. Blood. 2006; 107:528–34. [PubMed: 16189276]
4. Chion CKNK, Doggen CJM, Crawley JTB, Lane DA, Rosendaal FR. ADAMTS13 and von Willebrand factor and the risk of myocardial infarction in men. Blood. 2007; 109:1998–2000. [PubMed: 17053057]
5. Nguyen TC, Carcillo JA. Understanding the role of von Willebrand factor and its cleaving protease ADAM TS13 in the pathophysiology of critical illness. Pediatr Crit Care Med. 2007; 8:187–9. [PubMed: 17353760]
6. Ruggeri Z, Mannucci P, Lombardi R, Federici A, Zimmerman T. Multimeric composition of factor VIII/von Willebrand factor following administration of DDAVP: implications for pathophysiology and therapy of von Willebrand's disease subtypes. Blood. 1982; 59:1272–8. [PubMed: 6805532]
7. Chandler WL, Peerschke EIB, Castellone DD, Meijer P. Von Willebrand factor assay proficiency testing: the North American Specialized Coagulation Laboratory Association experience. Am J Clin Pathol. 2011; 135:862–9. [PubMed: 21571959]
8. Marques MB, Fritsma GA. Von Willebrand disease laboratory diagnosis: the saga continues. Am J Clin Pathol. 2011; 135:818–20. [PubMed: 21571953]
9. Magde D, Elson E, Webb WW. Thermodynamic fluctuations in a reacting system: measurement by fluorescence correlation spectroscopy. Phys Rev Lett. 1972; 29:705–8.
10. Magde D, Elson EL, Webb WW. Fluorescence correlation spectroscopy. 2. Experimental realization. Biopolymers. 1974; 13:29–61. [PubMed: 4818131]

11. Elson E, Magde D. Fluorescence correlation spectroscopy. I. Conceptual basis and theory. Biopolymers. 1974; 13:1–27.
12. Janzen J, Elliott TG, Carter CJ, Brooks DE. Detection of red cell aggregation by low shear rate viscometry in whole blood with elevated plasma viscosity. Biorheology. 2000; 37:225–37. [PubMed: 11026942]
13. [Accessed April 2012] Applications manual LSM 510 - Confocor 2: fluorescence correlation spectroscopy. Carl Zeiss Advanced Imaging Microscopy; 2001. http://www.bic.wur.nl/NR/rdonlyres/7E60452F-336F-4221-9C62-F5B713E64414/141218/Confocor2Manual.pdf
14. Favaloro EJ. An update on the von Willebrand factor collagen binding assay: 21 years of age and beyond adolescence but not yet a mature adult. Semin Thromb Hemost. 2007; 33:727–44. [PubMed: 18175279]
15. Smejkal GB, Shainoff JR, Kotte-Marchant KM. Rapid high-resolution electrophoresis of multimeric von Willebrand factor with a thermopiloted gel apparatus. Electrophoresis. 2003; 24:582–7. [PubMed: 12601725]

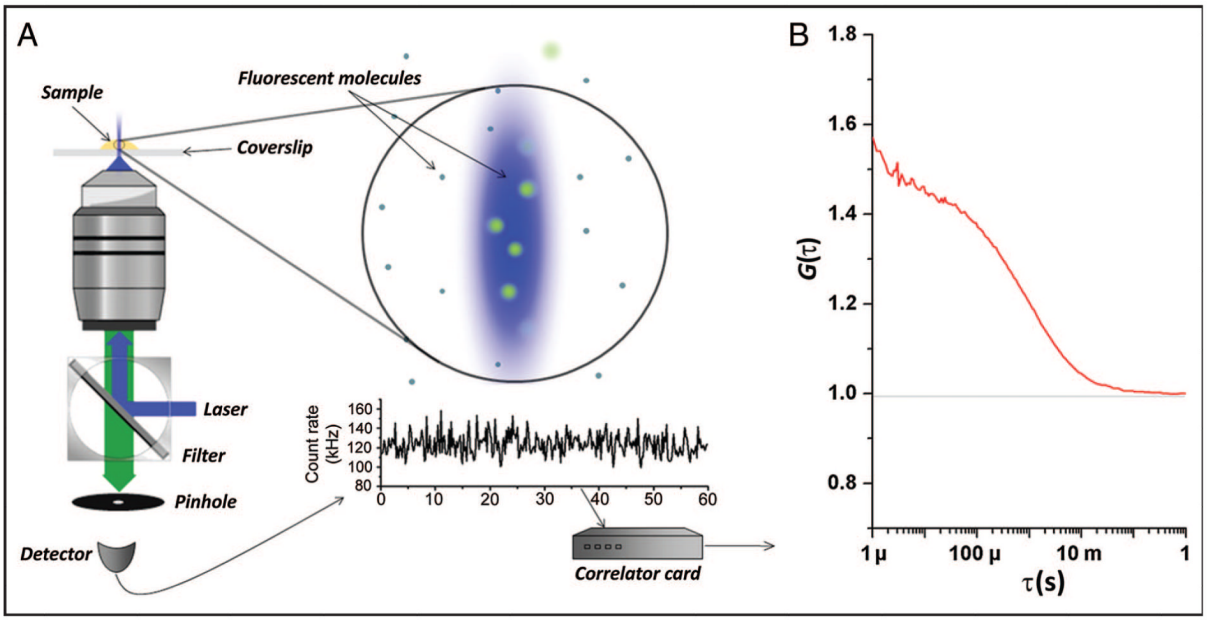

Fig. 1. Fluorescence correlation spectroscopy: setup and FCS curve

(A), Typical FCS setup. Excitation light (blue) from a laser reflects off the dichroic mirror and is focused by an objective lens. Fluorescent molecules are excited in the observation volume, and emitted light (green) is collected and directed toward the detector. Signal from the detector is autocorrelated by the correlator card. The output generated is an FCS curve. (B), Typical FCS curve. The autocorrelation variable, $G(\tau)$, is plotted as a function of the correlation time, τ. The curve can be fitted to a statistically derived model of fluctuations. $G(0)$ is the extrapolated value of G at $\tau = 0$, inversely proportional to the number of molecules in the observation volume and therefore concentration. The time at which $G(\tau)$ is roughly one-half of $G(0)$ is the mean residence time in the observation volume.

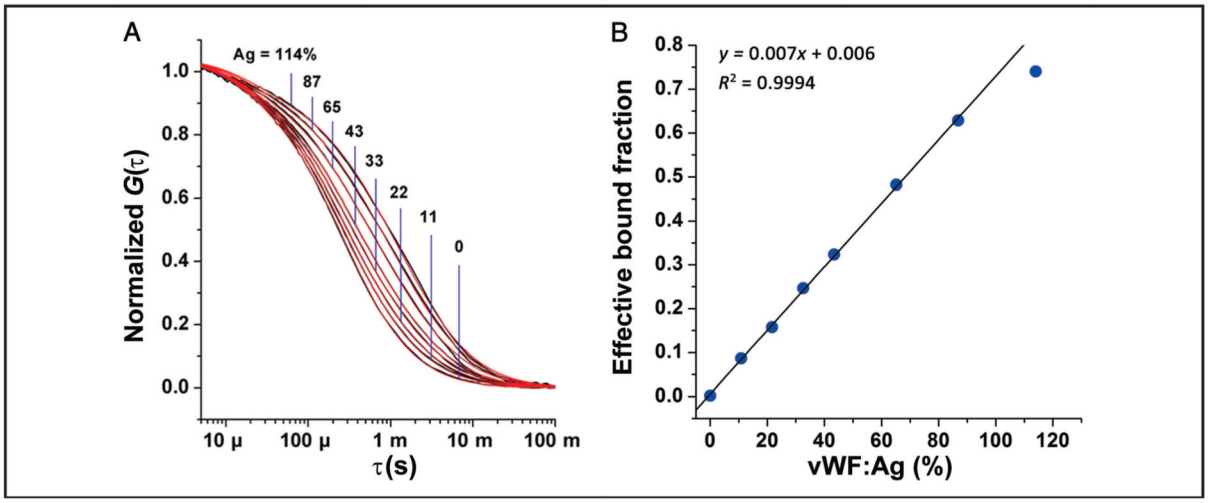

Fig. 2. vWF:Ag dilution study

(A), Correlation curves from dilutions of a healthy control (—, black) show a progressive shift to shorter diffusion times at lower antigen concentrations (each curve is labeled with corresponding vWF:Ag concentration in % units). A global fit to a 2-component standard FCS equation with the fast-diffusing component fixed at the τ_d of the free antibody is shown as red lines (—), which largely overlap the black correlation curves. (B), The resulting effective bound fraction component, plotted against the actual vWF:Ag concentration (%), shows a near-perfect linear correlation for antigen concentrations from 0% to 90%, beyond which the bound fraction component approaches total antibody concentration.

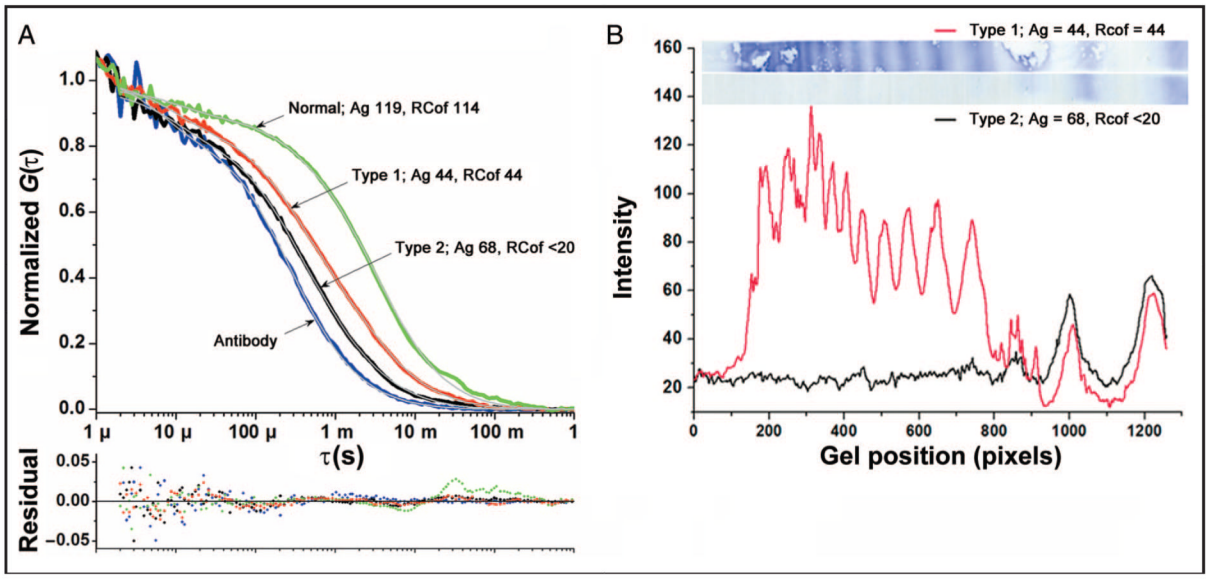

Fig. 3. Comparison of representative type 1 and type 2 samples

(A), Owing to the differences in multimer distribution, the FCS curve from a sample with type 1 vWD (red) is shifted to the right compared to a sample with type 2 vWD (black), despite the lower vWF:Ag concentration of the type 1 vWD sample. Both lie between a representative normal sample (green) and antibody alone (blue). (B), Multimer gels (top) show marked differences in multimer size distribution, which correspond qualitatively to activity differences. Densitometry of these samples, however, does not yield values that correspond to differences in total antigen despite being run on the same gel, a common limitation of multimer gel electrophoresis (type 1/type 2 background subtracted total intensity ratio = 2.7, differs from vWF:Ag ratio = 0.6).

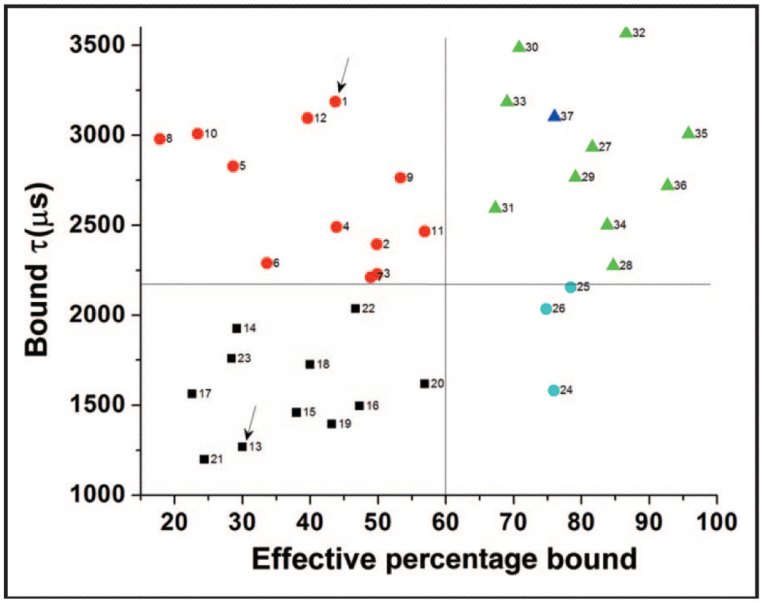

Fig. 4. Identification and classification of vWD with 2-component FCS fits

Type 1 vWD patients (●) have a distribution of mean diffusion times that overlaps that of samples with vWF within reference intervals (▲), but with a significantly reduced effective bound fraction, reflecting reduced amounts of a relatively normal distribution of multimers in type 1 vWD. Type 2 vWD patients have an effective bound fraction component that overlaps that of type 1 vWD patients but with a reduced diffusion time, reflecting a lack of large multimers (■). Three samples with high vWF:Ag but abnormal multimer analysis lacking large multimers (●) show a high effective bound fraction and short mean diffusion time. Two of these samples have been classified clinically as acquired vWD. The type 1 and type 2 vWD samples shown in Fig. 3 are denoted by arrows. The 4-h post-DDAVP sample described in Fig. 5 is also shown for reference (▲).

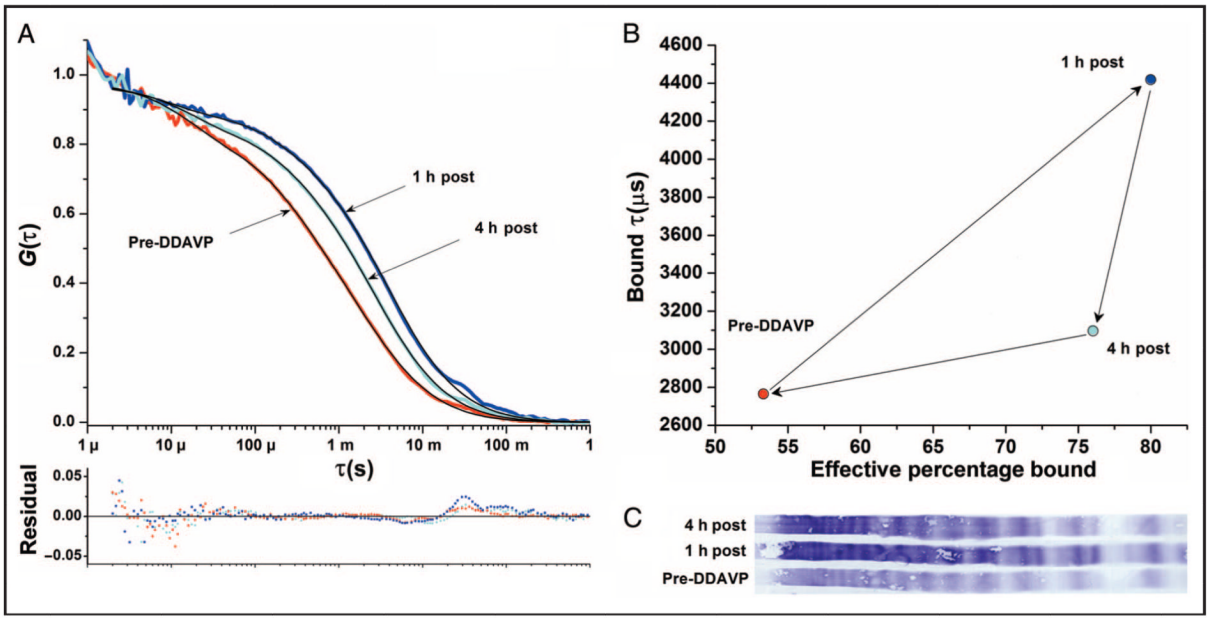

Fig. 5. FCS analysis of DDAVP trial in a type 1 vWD patient

(A), FCS curve shows a marked shift to longer diffusion time 1 h post-DDAVP (post). After 4 h, the FCS curve shows a partial return toward baseline. The FCS curves and residuals show a bump at long τ due to large particles that become more pronounced in the samples post-DDAVP. (B), Two-component fit analysis at 1 h is consistent with the release of primarily large multimers, with an increase in both calculated total quantity and mean multimer size on the basis of mean bound diffusion time. At 4 h, the fit suggests the breakdown of large multimers, with a decrease in the mean bound diffusion time but less decrease in the percentage of antibody bound. (C), The corresponding multimer gel containing these 3 samples is shown for comparison. Traditional testing values for these samples were (Ag/RCof/FVIII): pre-DDAVP = 48/48/69, 1 h = 115/165/151, 4 h = 83/105/109.

Table 1

Characteristics of vWD samples subsequently tested by FCS.

Sample	Antigen, %	RCoF, %	Factor VIII, %	Multimer analysis	Type
1	44	44	43	All multimers present in decreased amounts	Type 1
2	43	28	38	All multimers present in decreased amounts	Type 1
3	43	40	53	All multimers present in decreased amounts	Type 1
4	45	42	73	All multimers present in decreased amounts	Type 1
5	39	<20	42	All multimers present in decreased amounts	Type 1/2M
6	13	<20	13	All multimers present in decreased amounts	Type 1
7	43	40	63	All multimers present in decreased amounts	Type 1
8	15	<20	48	All multimers present in decreased amounts	Type 1
9	48	48	69	All multimers present in decreased amounts	Type 1
10	37	26	26	All multimers present in decreased amounts	Type 1
11	38	42	78	All multimers present in decreased amounts	Type 1
12	32	25	37	All multimers present in decreased amounts	Type 1
13	68	<20	14	No large or intermediate multimers	Severe type 2A
14	31	<20	39	Absence of large multimers	Type 2A
15	19	<20	39	Absence of large multimers	Type 2A
16	50	<20	41	Absence of large multimers	Acquired type 2
17	21	<20	31	Absence of large multimers	Type 2A
18	17	<20	31	Absence of largest multimers	Type 2A
19	41	<20	103	Absence of largest multimers	Mild type 2A
20	77	35	65	Absence of large multimers	Acquired Type 2
21	38	18	29	Absence of large multimers	Type 2A
22	51	28	72	Absence of large multimers	Acquired type 2?
23	31	<20	39	Absence of large multimers	Type 2A
24	100	39	74	Absence of large multimers	Type 2
25	146	62	132	Absence of large multimers	Acquired type 2
26	188	121	112	Absence of largest multimers	Mild acquired type 2